

FEA simulation of a movable side trowel for an extrusion and deposition mechanism with a ceramic material

Hong-Kyu Kwon*

Industrial and Management Engineering, Namseoul University, Chonan, South Korea

This paper presents our experimentation and modeling efforts to study the effect of pivoting a side trowel with a ceramic as the fabrication material. Using FEA simulations, we derived certain basic understandings of the effect and motion of pivoting the side trowel. We found that two side trowels are most aptly suited, both in terms of delivering the optimal fusion between layers while fabricating true 3D geometry. Our experiments validate these results.

Key words: Finite Element Analysis (FEA), Extrusion, Deposition, Orifice, Movable Side Trowel.

Introduction

Contour crafting (CC) is an additive fabrication process developed at the University of Southern California [1]. The CC process somewhat resembles a mold-filling operation in that clay is being packed under pressure resulting from the contact with the semi-solid base layers and the trowels. Troweling is the chief surface formation mechanism in CC. The final surface finish will rely on the pressure at the deposition point for the trowel to smooth out the surface, and the flow pattern of the material as a result of that pressure. Besides, the material undergoes a 90 °C rotation immediately after extrusion.

As shown in Fig. 1. the basic CC process consists of an extrusion orifice, two perpendicular solid planar surfaces formed by a top trowel and a side trowel. The side trowel



Fig. 1. CC machine (340*380*210mm) with the movable side trowel for fabricating complex 3D part.

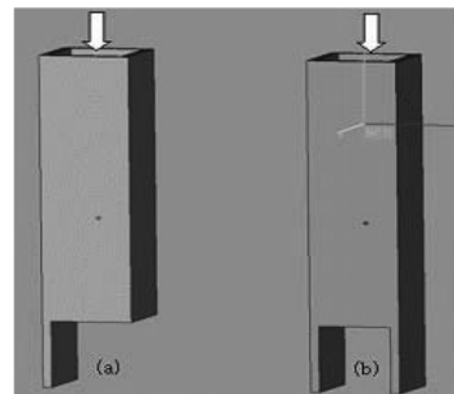


Fig. 2. Side trowel (5*5*2 mm) designs used in experiments.

smooths out and shapes the external surface of a CC-fabricated part in order to achieve the desired geometric profile and surface finish. The length of the side trowel may extend beyond the thickness of an individual layer of the fabricated part and slightly overlap with the previous layer.

Specifically, we considered the effects of the following two types of side trowel shown in Fig. 2. (a) single side, and (b) double side trowel, respectively. We undertook simple process modeling described in the following section for understanding the process flow characteristics.

Material characteristics

Here, we studied CC with specific reference to cylindrical clay geometries. The composition of the material is shown in Tables 1 and 2.

The components of the clay exhibit highly plastic properties with very high shear rates. The deflocculants¹

¹A deflocculant is a source of ions that charge clay particles to repel each other electrostatically, thus producing a slurry with a faster flow rate at minimum viscosity.

*Corresponding author:
Tel : +82-041-580-2206
Fax: +85-041-580-2906
E-mail: hongkyuk@nsu.ac.kr

Table 1. Clay

Pioneer Talc	3402 gm
Taylor Ball clay	2268 gm
Barium carbonate	7 gm
Soda Ash	7.5 gm
Sodium silicate	0.3oz (Deflocculant)
Water	>0.8[Gallons]

Table 2. Taylor Ball clay

SiO ₂	62.90%	CaO	0.09%
Al ₂ O ₃	23.70%	Na ₂ O	0.09%
Fe ₂ O ₃	1.07%	K ₂ O	0.35%
TiO ₂	1.58%	LOI	9.58%

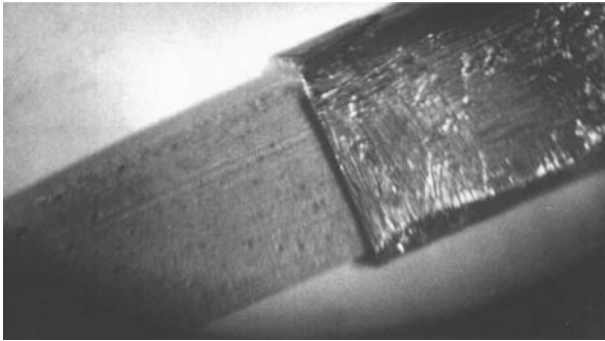


Fig. 3. Extrudate exhibiting no orifice swell with nozzle size (5*5*20 mm).

render the clay to be almost Bingham [2]. The Bingham properties of the clay body give it an internal structure that collapses above a yield stress and above which rheological behavior is linear. This linear behavior allows us to model the flow domain as a Newtonian fluid [3, 4].

Further examination of the clay properties revealed that the clay did not swell upon exiting the orifice, probably due to its readiness to shear and virtual absence of an elastic phase. Thus super-plasticity is demonstrated as shown in Fig. 3.

Governing Relationships

Process parameters

In addition to the large number of process parameters that exist in a basic extrusion system, additional parameters are involved in the CC process. Because of this complexity, some preliminary experimentation was necessary to determine the process parameters.

Through several experimental investigations, an attempt was made to calibrate our input and output parameters, as well as to understand the behavior of the material during extrusion. The input parameters were extrusion rate (V_e) [mm/s], linear speed (V_r) [mm/s], thickness of the layer (h) [mm], diameter of the part (D) [mm], and

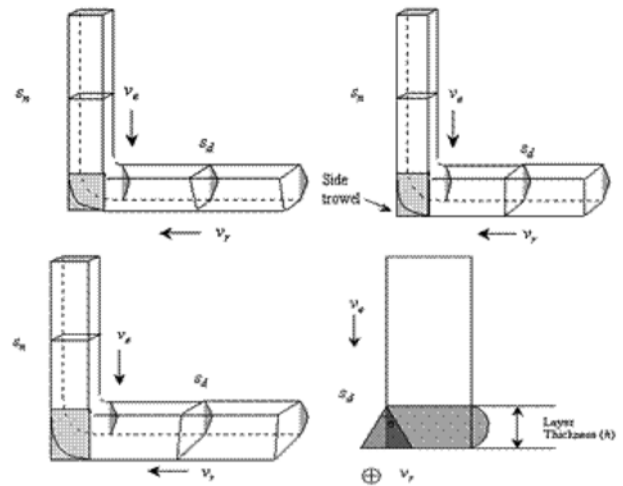


Fig. 4. Schematic view of steady flow.

number of layers (n). The output parameters considered were the vertical profile (Dh), and the surface roughness (R_a) which is the main response.

According to the mass balance principle, the material input is equal to its output. Thus, the following equations may be written:

$$S_d = C_d \frac{V_e S_n}{V_r} \quad (1)$$

$$S_d = S_d + \frac{1}{2} * h^2 * \tan(\theta) \quad (2)$$

where C_d is a constant ratio of material density or the compression factor

V_e (mm/s) is the extrusion velocity

V_r (mm/s) is the linear speed of the extrusion head

h (mm) is the height of the deposited layer

θ (degree) is the pivoting angle of the side trowel

S_n (mm²) is the cross sectional areas of the nozzle

S_d (mm²) is the cross sectional areas of deposited layer

S_d' (mm²) is the cross sectional areas of deposited layer when $\theta = 0$

V_e will always increase at the deposition point because the extrudated material is partially unbound after the exit of the nozzle. Hence, S_d will increase at the point if other parameters are constant. As shown in Fig. 4. S_d also relies on an angle of the side trowel and the pressure at the deposition point which mainly affect the surface roughness of fabricated parts.

Assumption in FEA modeling

As previously mentioned, the trowels and the orifice are part of the exit geometry and play a significant role in affecting the flow of the extrudate clay. The surface quality is also determined by a multitude of parameters like the design of the extrusion system, the material, the fluid properties, and the test parameters (variants of the system). Furthermore, we used the material property values consistent with those of a Bingham fluid in our

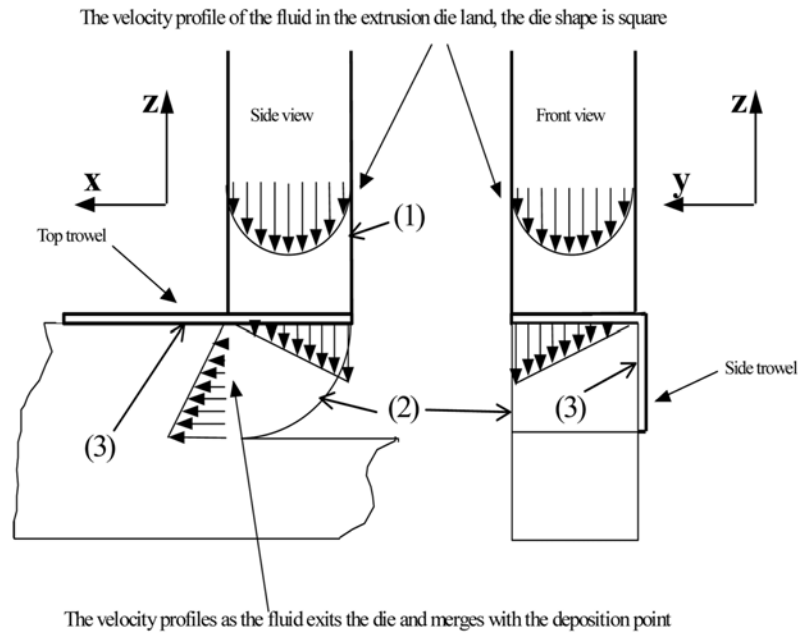


Fig. 5. Schematic of material flow in CC.

analysis. This is because the clay that we used in our studies behaves like a Bingham fluid.

Analysis of any non-Newtonian flow is very complicated. However, the following assumptions were introduced in order to facilitate the finite element modeling and analysis. The flow in its steady state condition exhibits linear rheological properties as a result of the effect of the deflocculant additives [2, 5, 6]. The compressibility of the clay is neglected, and the flow is assumed to be a single phase, isothermal and laminar [7, 8]. Making use of these assumptions, the linearized governing flow equations can be described by:

$$\frac{\partial}{\partial x}(\rho u) + \frac{\partial}{\partial y}(\rho v) + \frac{\partial}{\partial z}(\rho w) = 0 \quad (3)$$

$$\frac{\partial}{\partial z} \left(\eta \frac{\partial u}{\partial z} \right) - \left(\frac{\partial P}{\partial x} \right) = 0 \quad (4)$$

$$\left(\frac{\partial}{\partial z} \right) \left(\eta \frac{\partial v}{\partial z} \right) - \left(\frac{\partial P}{\partial y} \right) = 0 \quad (5)$$

where η is the viscosity, P is the pressure, ρ is the density, and u , v , and w are the velocities in the x , y , and z directions at the boundary condition ($u = 0$, $v = V_x$, and $w = V_z$). With these assumptions FEA simulation is detailed in the following subsection.

Boundary conditions in FEA modeling

The solution domain shown in Fig. 5. is defined by four boundaries: the die land wall (1), the free surface boundary (2), and the walls of the trowel (3). The governing equations of mass, momentum, and energy are combined with the above boundary conditions. For the momentum equations the velocities are specified along the boundary. For the energy equation, the conditions are set isothermally ones. The prescribed conditions at these boundaries are:

(1) The die-land wall: Under constant flow rate the velocity profile of the material is parabolic with a constant magnitude.

(2) The free surface boundary: The free surface boundary conditions are based on the requirement that no momentum flux may cross the free surface of the fluid. The stress tensors normal and tangential to the free surface are 0.

(3) The walls of the trowel: At the walls of the trowel a no-slip boundary condition is applied; the velocity components, both tangential and normal to the wall vanish there.

FEA modeling Post-processing

A commercial CFD package was also used for simulating the side trowel angle. To form a computational grid as shown Fig. 6. the flow domain was subdivided into a number of cells. After the grid generation, six boundary conditions were specified: trowel walls and orifice walls, an inlet boundary, free surface boundaries, a moving bottom layer, and an outlet boundary. The same as the Orifice simulation, the viscosity (η) measured in terms of the damping ratio and density (ρ) were set at 15%, and 24 kN/m³ respectively. The flow was considered to be laminar and isothermal.

FEA simulation

Figure 7(a) shows the flow profiles of the particulate flow with the exterior angle at conditions (η is 15%, ρ is 24 kN/m³, and u is 0 mm/s, v is 2.112 mm/s, w is 4 mm/s). As shown in Fig. 8(a). the flow profiles of the particulate flow with the interior angle are at conditions (η is 15%, ρ 24 kN/m³, and u is 0 mm/s, v is 1.471 mm/s, w is 4 mm/s). The flow profiles of the particulate flow

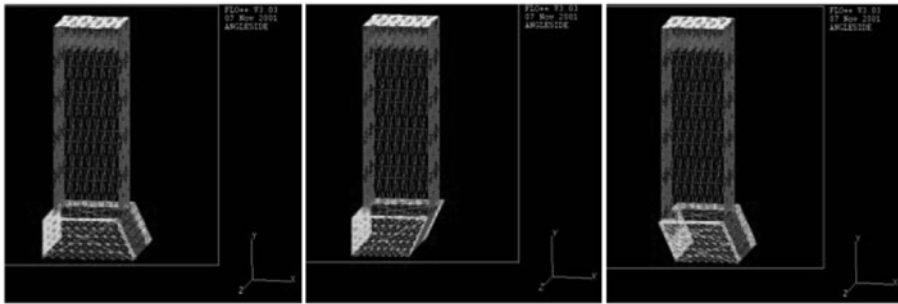


Fig. 6. Grid structure for (a) an exterior angle, (b) an interior angle, and (c) two side trowels.

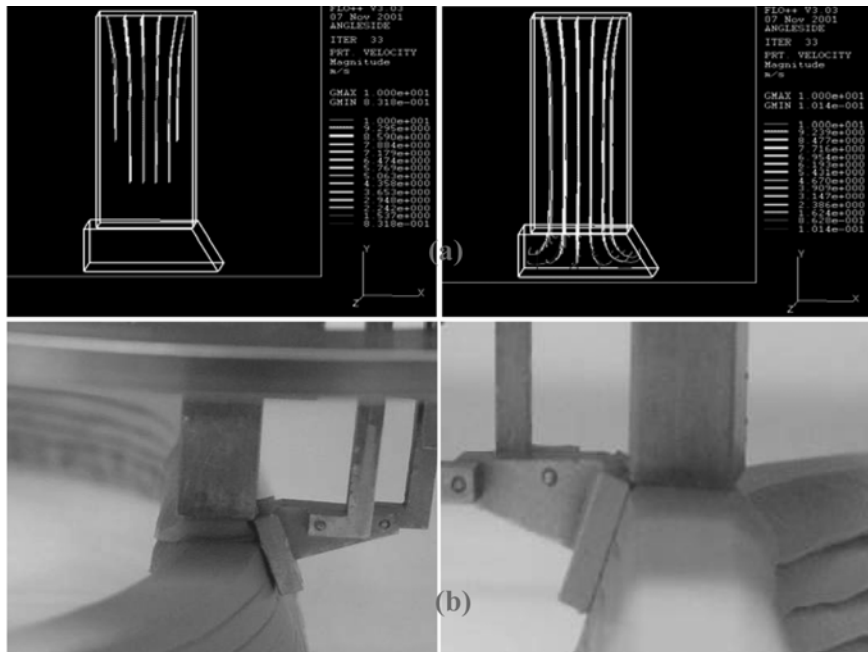


Fig. 7. A flow line with an exterior angle with layer height (2.5 mm) (a) Simulation; (b) Actual process.

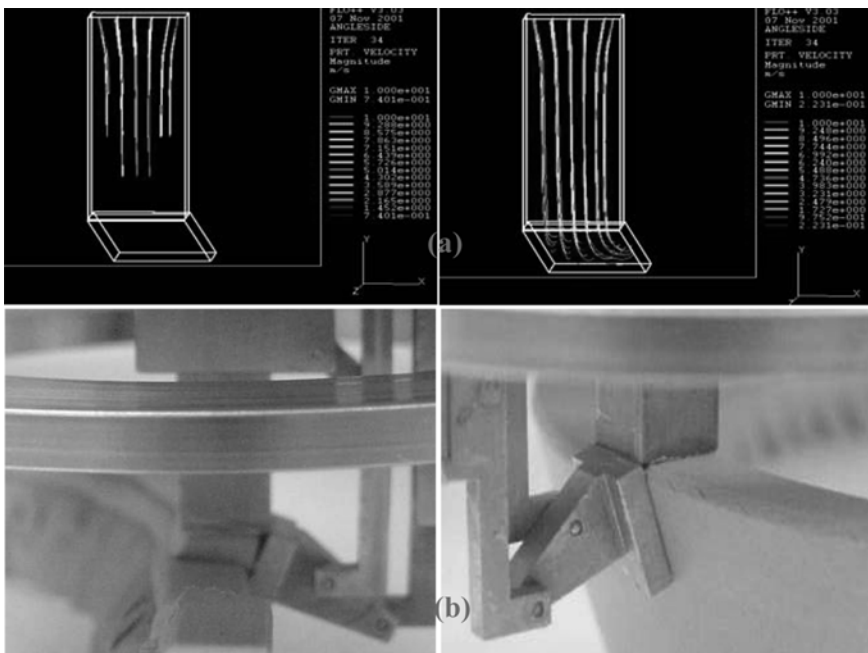


Fig. 8. A flow line with an interior angle with layer height (2.5 mm) (a) Simulation, (b) Actual process.

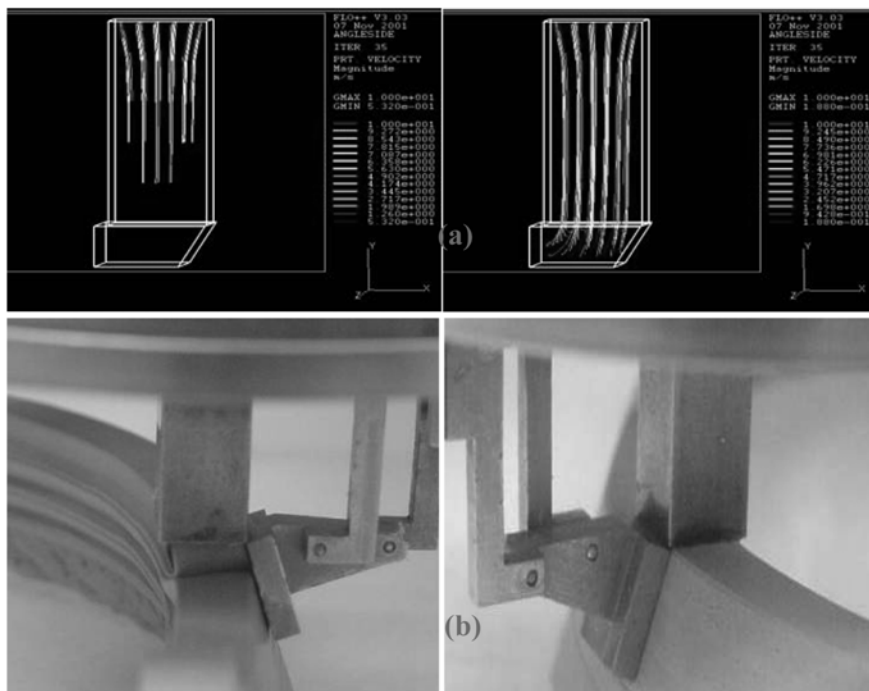


Fig. 9. A flow line with two side trowel with layer height (2.5 mm) (a) Simulation; (b) Actual process.

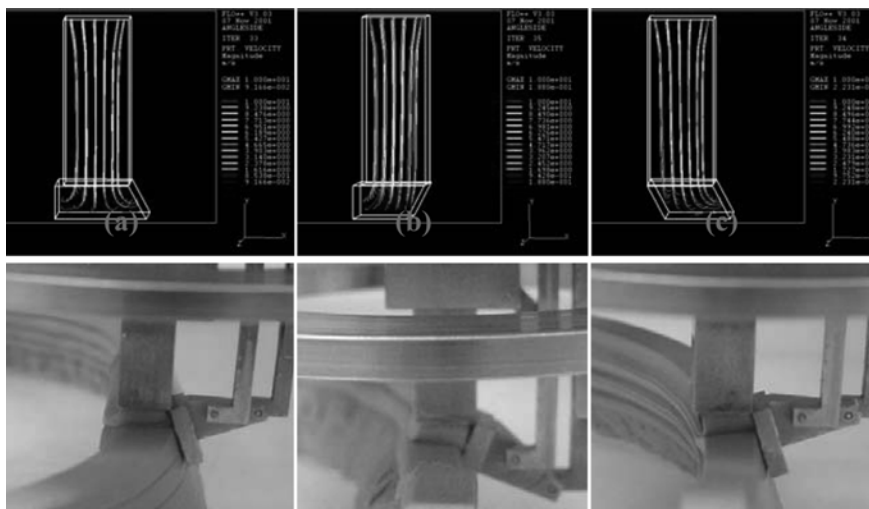


Fig. 10. Comparison with the partial lines with layer height (2.5 mm) (a) Exterior, (b) Interior; (c) Two side trowels.

with the two side trowels in Fig. 9(a). are at the conditions (η is 15%, ρ is 24 kN/m³, and u is 0 mm/s, v is 2.188 mm/s, w is 4 mm/s).

As shown in these simulation results, the complex flow conditions occurred in the flow domain. Since the friction at the boundary, especially the walls, retards the flow, the flow in the center of the nozzle is much more rapid. Also, the flow patterns are changed on the deposited point relating to the side trowel angle, which explains why we get the different flow profile.

The photographs of a CC taken on-line, shown in Fig. 7(b). with the exterior angle, confirm the results obtained by the simulation in Fig. 7(a). The photographs of a CC taken on the actual process, shown in Fig. 8(b).

with the interior angle, confirm the results obtained by the simulation obtained by the simulation in Fig. 8(a). The photographs of a CC taken on the actual process, shown in Fig. 9(b). with the two-side trowel, confirm the results obtained by the simulation in Fig. 9(a).

Discussions

Comparison with flow profile

To achieve desirable surface quality, the process parameters are optimized under each of the three different conditions. As shown in the Fig. 10(a), the material is dispersed symmetrically in and outward on the bottom phase. Hence, it might be difficult to fill the material

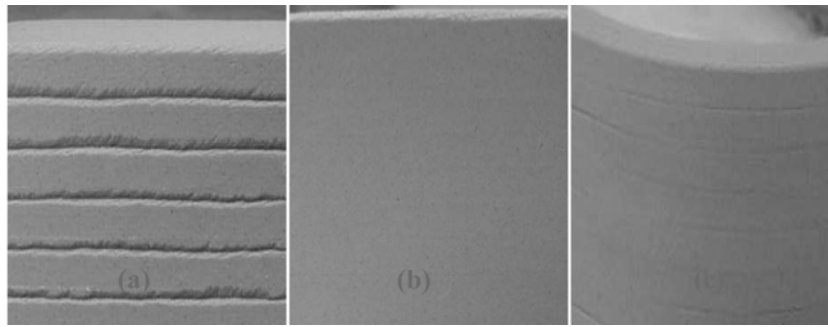


Fig. 11. Surface quality of fabricated parts with layer height (2.5 mm) (a) Exterior; (b) Interior; (c) Two side trowels.

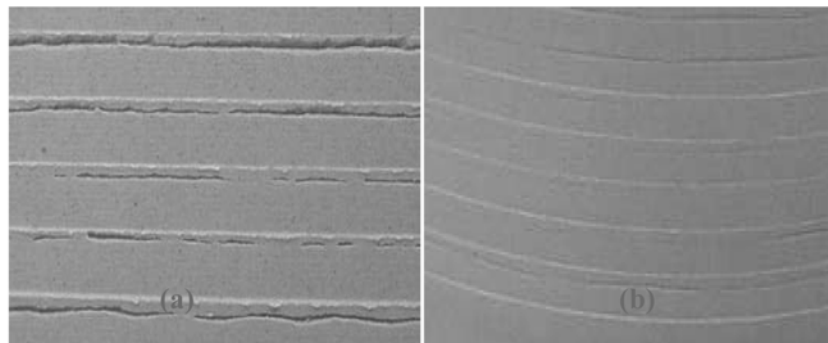


Fig. 12. Surface finish at the near optimal condition with an exterior angle: (a) below-optimal condition, (b) over-optimal condition.

into the corners. Owing to the inside trowel, the flow pattern is changed as shown in Fig. 10(c). The material tends to flow outwards where the outside trowel is. This design might be better to fill the material into the corners, and to achieve a better surface finish of the fabricated part as shown in Fig. 11(c). When the angle of the side trowel is interior as shown in Fig. 10(b), the material is directly deposited on the side trowel, and then pushed inwards. Hence, the corners are going to be filled completely, and the perfect surface quality is achieved as shown in Fig. 11(b).

Surface quality

By smoothing out the presence of unfilled regions between the consecutive layers at the exterior angle in Fig. 11(a), higher velocities were needed in order to achieve a near equal surface roughness value. However, if the extrusion pressure on the deposited point was increased beyond an optimum value to fill up these voids, it would cause a loss of the desired geometric profile, thus deteriorating the surface quality as shown in Fig. 12.

Conclusions

The simulation program results play an important role in gaining a better insight into the flow process. They enable the prediction of the consequences of variations

in boundary conditions, different angles of the side trowel and changes in other flow parameters of the process and material. The experimental results form a basis to come to the conclusion that the results obtained with the two side trowels were the best, even when we consider the trade-off between using extrusion pressures high enough for the layers to fuse with each other with a uniform flow pattern, and low enough to avoid distortion of the part (maintaining the geometric profile).

References

1. B. Khoshnevis, *Materials Technology* 13[2] (1998) 52-63.
2. D. Ding, P. Townsend and M.F. Webster, in *Proceedings of IUTAM Symposium on Numerical Simulation of Non-Isothermal Flow of Viscoelastic Liquids*, November 1993 (Kerkrade Netherlands, 1993) p. 121.
3. J. Bardet, "Experimental Soil Mechanics" (Prentice-Hall, 1997) p. 31.
4. R.F. Craig, "Soil Mechanics" (E & FN Spon, 1997) p. 38.
5. R.W. Fox and A.T. McDonald, "Introduction to fluid mechanics" (John Wiley & Sons, Inc., New York, 1985) p. 50.
6. D.H. Han, "Multiphase Flow in Polymer Processing" (Academic Press, New York, 1981) p. 85.
7. D.G. Baird and D.I. Collias, "Polymer Processing Principles and Design" (John Wiley & Sons, Inc., New York, 1998) p. 45.
8. J. Benbow and J. Bridgwater, *Paste Flow and Extrusion* (Oxford, 1993) p. 24.